



TITLE:

Studies on the Power Requirement of Mixing Impellers (III) : Empirical Equations for Paddle Agitators in Cylindrical Vessels

AUTHOR(S):

NAGATA, Shinji; YOKOYAMA, Tōhei; MAEDA, Hiroyuki

CITATION:

NAGATA, Shinji ...[et al]. Studies on the Power Requirement of Mixing Impellers (III) : Empirical Equations for Paddle Agitators in Cylindrical Vessels. *Memoirs of the Faculty of Engineering, Kyoto University* 1956, 18(1): 13-29

ISSUE DATE:

1956-03-15

URL:

<http://hdl.handle.net/2433/280342>

RIGHT:

Studies on the Power Requirement of Mixing Impellers (III)

—Empirical Equations for Paddle Agitators in Cylindrical Vessels.—

By

Shinji NAGATA, Tōhei YOKOYAMA and Hiroyuki MAEDA

Department of Chemical Engineering

(Received November 24, 1955)

1. Introduction.

Paddle agitators are most frequently used in chemical industries, because of the simplicity of their design and construction. Nevertheless, the studies on their power requirements are not complete and their results not consistent.

Among them, the results obtained by J. H. Rushton and his co-workers¹⁾ are very extensive and most valuable. However, the relation between the power consumption and the ratio of paddle size to vessel diameter is not clarified. Also they emphasize the advantages of baffle plates and the results of the power consumption of paddles without baffles are not sufficient.

First of all, in this report, power requirements for the paddle agitators are studied, because it is easy to prepare paddles and to indicate their dimensions, and they are assumed to be the basic form of other impellers such as turbines or propellers.

2. General correlation of the power consumption for paddles.

2.1. Notations used (refer to Fig. 1.)

D	: Tank diameter	(m)
H	: Liquid depth	(m)
H_p	: Height of an impeller off bottom	(m)
	or the relative height off bottom (refer to Fig. 1)	(—)
d	: Impeller diameter	(m)
b	: Width of impeller blades	(m)
θ	: Angle of blades to horizontal plane	(—)
n_p	: number of blades of an impeller	(—)
N	: Impeller speed in r.p.m.	(1/min)
n	: Impeller speed in r.p.s.	(1/sec)

P	: Power consumption for agitation	(Kg·m/sec)
ρ	: Density of liquid	(kg/m ³)
μ	: Viscosity of liquid	(kg/m·sec)
w	: Width of baffle plates	(m)
n_B	: Number of baffle plates	(-)
g	: Gravitational constant	(m/sec ²)
g_c	: Gravitational conversion factor	(kg·m/Kg·sec ²)

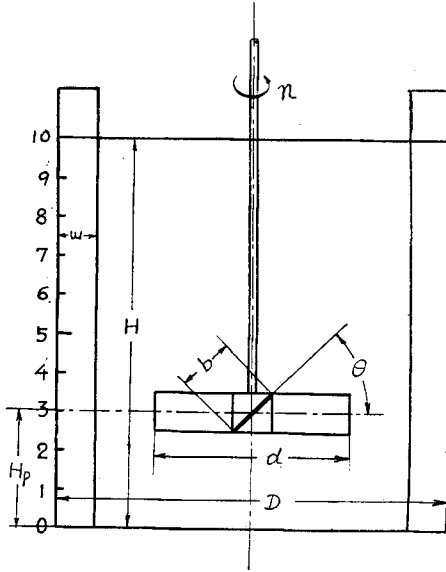


Fig. 1. Schematic diagram of impellers and vessels.

2. 2. Basic dimensionless equation.

$$\frac{Pg_c}{\rho n^3 d^5} = \left(\frac{d^2 n \rho}{\mu} \right)^p \left(\frac{dn^2}{g} \right)^q f \left(\frac{d}{D}, \frac{b}{D}, \frac{H}{D}, \theta \right) \quad (1)$$

where

$$\frac{Pg_c}{\rho n^3 d^5} = N_P : \text{Power number}$$

$$\frac{d^2 n \rho}{\mu} = R_e : \text{Reynolds number in an agitated system.}$$

$$\frac{dn^2}{g} = F_r : \text{Froude number in an agitated system.}$$

Among these, the Froude number should be taken into consideration when the system has a free surface and this term can be taken as a constant from the results of a previous paper²⁾ and also from those mentioned later. As the exponent q in

Eq. (1) is a small decimal, the values of $(dn^2/g)^q$ is nearly equal to 1.0 regardless of the magnitude in (dn^2/g) .

For a while, let the case be considered when the liquid depth is equal to the tank diameter ($H=D$) and the paddle is installed at half the liquid depth ($H_p=H/2$) perpendicularly to the horizontal plane ($\theta=90^\circ$).

Then Eq. (1) becomes.

$$\frac{Pg_c}{\rho n^3 d^5} = \left(\frac{d^2 n \rho}{\mu} \right)^p f \left(\frac{d}{D}, \frac{b}{D} \right) \quad (2)$$

3. Conditions of experiments.

3. 1. Dynamometers.

The dynamometers used for the power measurement are No. 2A and No. 3 (No. 1 in some cases) which are precisely explained in a previous report.²⁾

3.2. Impellers.

Experiments are carried out with the paddle agitators having the following dimensions in diameter d and width b and composed of two blades ($n_p=2$),

$$d/D = 0.3, \quad 0.4, \quad 0.5, \quad 0.7, \quad 0.8, \quad 0.9$$

$$b/D = 0.05, \quad 0.1, \quad 0.2, \quad 0.3, \quad 0.7, \quad 0.9$$

3.3. Vessels or Tanks.

The vessels used for these experiments are cylindrical in shape having flat bottoms, the sizes of which are shown in Table 1.

Table 1. Vessels used

Vessel number	Diameter of Vessel (cm)	Materials	Volume (l) H=D
1	117	steel	1,260
2	58.5	stainless steel	158.5
3	30.0	Aluminium	21.2
4	23.4	glass	10.1
5	15.0	glass	2.65

3.4. Liquid used.

Water, machine oils with various viscosities, and millet-jelly, having viscosities ranging from 10^3 to 10^4 c. p. or more, are used. Viscosity of the liquids used is measured by the Brookfield rotating viscometer.

4. Results obtained.

To begin with, the paddle length is made constant and its width varied in the range of $b=0.05D \sim 0.9D$, and the power consumptions P in the liquids of various viscosities are determined in a wide range of agitator speeds.

The results of these experiments are summarized by the term $N_P = (Pg_c/\rho n^3 d^5)$ versus $Re = (d^2 n \rho / \mu)$ on a logarithmic paper. Fig. 2 shows $d=0.8D$ in the upper, $d=0.5D$ in the middle, and $d=0.3D$ in the lower group of curves.

Next, the paddle width is made constant and its length varied in the range of $d=0.3D \sim 0.9D$. The results of these experiments are shown by Fig. 3; $b=0.2D$ in the upper and $b=0.05D$ in the lower group of curves. These curves can be classified into the following three ranges;

- (1) In the range of high viscosities (Re is less than $10 \sim 10^2$), the slope of the curves is nearly equal to -1 .
- (2) In the range of medium viscosities (Re is greater than $10 \sim 10^2$ and smaller than $10^4 \sim 10^5$) the slope of the curves varies widely with (b/D) ratio and slightly with (d/D) ratio.

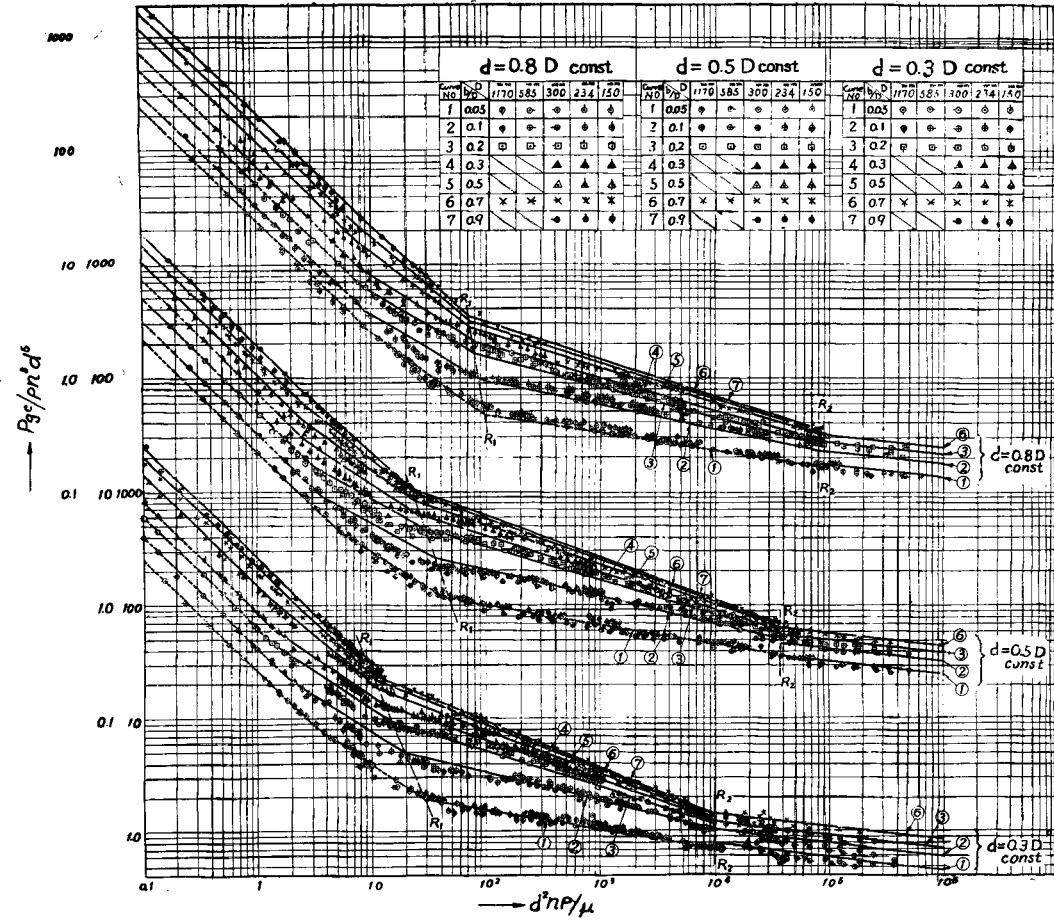


Fig. 2. Relation between power number and Reynolds number for paddles having various width.

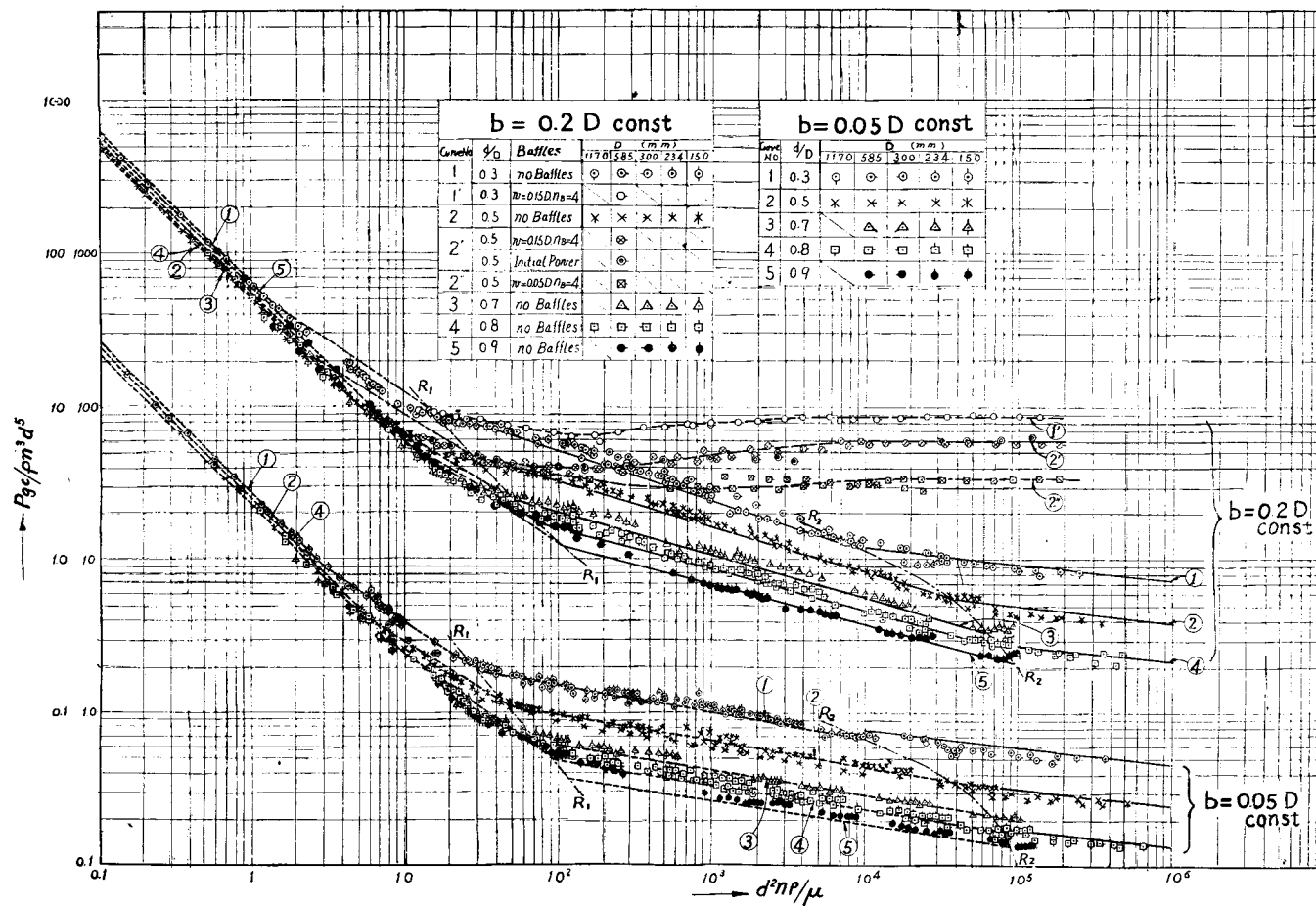


Fig. 3. Relation between power number and Reynolds number for paddles having various length.

(3) In the range of low viscosities (Re is greater than $10^4 \sim 10^5$), the slope of the curves is nearly constant.

The authors intend to derive empirical equations corresponding to these three ranges. R_1 and R_2 are the boundary Reynolds number shown by the chain line in Fig. 2 and 3 and they are calculated by Eq. (14) and (15) respectively.

4.1. Power equation for high viscosity range.

$$(Re < 10 \sim 10^2 \text{ or more exactly } Re < R_1)$$

In the range of $Re < R_1$, the exponent p is nearly equal to -1 (refer to the plots in Fig. 2 and 3).

Then Eq. (2) becomes.

$$\Phi = \left(\frac{Pg_c}{\rho n^3 d^5} \right) \cdot \left(\frac{d^2 n \rho}{\mu} \right) = \frac{Pg_c}{\mu n^2 d^3} = f \left(\frac{d}{D}, \frac{b}{D} \right) \quad (3)$$

As the term Φ is a function of (d/D) and (b/D) , the values of N_P in $Re=1$ in Fig. 2 and 3 are equal to Φ and they are taken and plotted against (b/D) as shown

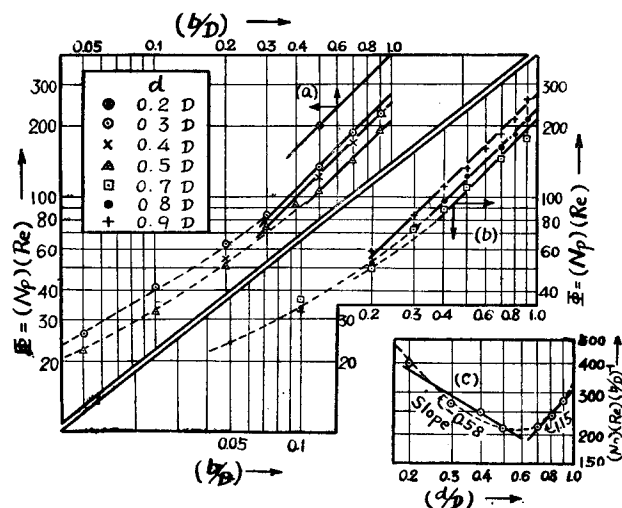


Fig. 4. Effect of (b/D) and (d/D) ratios for power number in laminar flow range.

by Fig. 4. The plots of Φ versus (b/D) are curved in the range where (b/D) is less than 0.3; but in the range of greater (b/D) , it can be approximated by a straight line having a slope of 45° . Then, for the range of $(b/D) > 0.4$, Eq. (4) is obtained.

$$\Phi(b/D)^{-1} = f'(d/D) \quad (4)$$

$\Phi(b/D)^{-1}$ values are plotted against (d/D) as shown by the curve (c) in Fig. 4.

As a rule, in the mixing of liquids of high viscosities,

the paddles of larger sizes in d and b should be used as will be reported later. Therefore, let the equation be limited to the paddles that have larger sizes in d and b . Then, from the plots in Fig. 4 (c) the following equation is obtained for the range of application; $(d/D) = 0.7 \sim 0.9$ and $(b/D) = 0.4 \sim 0.9$.

$$\frac{Pg_c}{\mu n^2 d^3} = 310 \left(\frac{b}{D} \right) \left(\frac{d}{D} \right)^{1.15} \quad (5)$$

4.2. Power equation for medium viscosity range.

$$(10 \sim 10^2 \leq Re \leq 10^4 \sim 10^6 \text{ or more exactly } R_1 \leq Re \leq R_2)$$

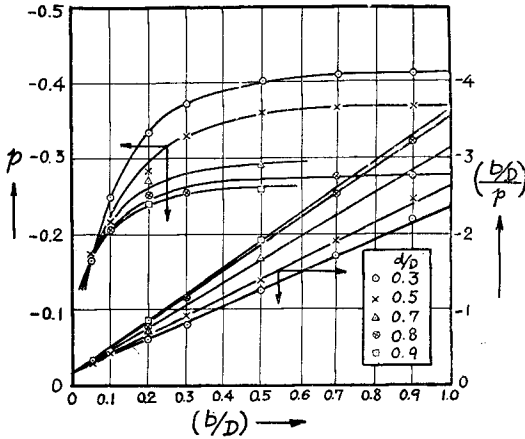


Fig. 5. Relation between the slope p in the medium viscosity range of Fig. 2. and the (b/D) ratio.

In the medium viscosity range, the exponent p for Reynolds term varies widely in a complicated manner.

The slopes p of N_P versus Re curves in Fig. 2 and 3 are taken for the paddles of various length d and width b and plotted against (b/D) in Fig. 5, taking (d/D) ratios as parameters. This relationship is replotted with $(b/D)/p$ as ordinate and (b/D) as abscissa and a straight line relationship is obtained;

$$p = \left[\frac{(b/D)}{\alpha + \beta(b/D)} \right] \quad (6)$$

In this equation, the coefficient α is equal to (-0.17) and the coefficient β varies considerably by the (d/D) ratios. The relation between β and (d/D) is not simple, but attaching importance to the ranges of $(d/D) = 0.3 \sim 0.5$, the following expression is adopted.

$$\beta = -\{1.8 + 1.37(d/D)\} \quad (7)$$

Thus, Eq. (6) is determined as follows:

$$p = - \left[\frac{(b/D)}{0.17 + \{1.8 + 1.37(d/D)\}(b/D)} \right] \quad (6')$$

By the same procedure used in the high viscosity range, the values of \mathcal{O}' are calculated and plotted against (d/D) ratio as shown by Fig. 6 (solid lines).

$$\mathcal{O}' = \left(\frac{Pg_c}{\rho n^2 d^5} \right) \cdot \left(\frac{d^2 n \rho}{\mu} \right)^{-p} = f' \left(\frac{d}{D}, \frac{b}{D} \right) \quad (8)$$

As shown by Fig. 6, $\log \mathcal{O}'$ is represented as a straight line against the (d/D) ratio:

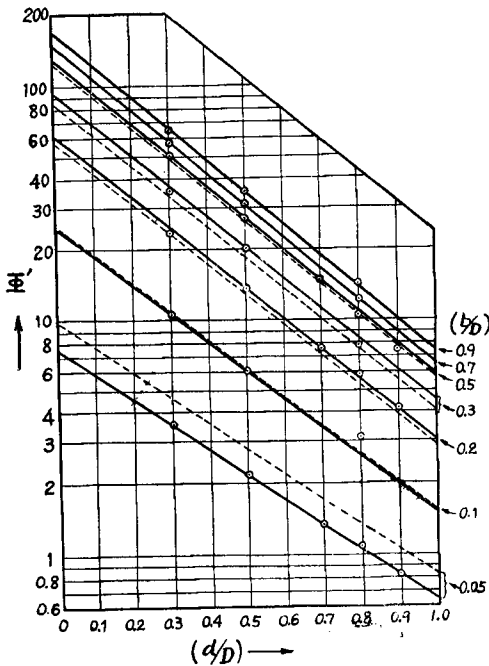


Fig. 6. Values of \mathcal{O}' vs (d/D) ratio—Comparison of the observed data (solid line) and those calc. by Eq. (9') (dotted line).

$$\log \Phi' = l - m (d/D) \quad (9)$$

The slopes m of the straight lines in this diagram differ slightly by the variation in (b/D) ratio and is represented by Eq. (10).

$$m = \left[\frac{(b/D)}{0.01 + 0.73 (b/D)} \right] \quad (10)$$

From Fig. 6, the ordinate values $\log \Phi'_0$ at $(d/D)=0$ are read off and, plotting it against (b/D) , then a hyperbolic relation is obtained as shown by Eq. (11).

$$l = \log \Phi'_0 = \left[\frac{(b/D)}{0.03 + 0.42 (b/D)} \right] \quad (11)$$

But at $(b/D)=0.05$, the observed values Φ'_0 are slightly different from those obtained by Eq. (11).

Therefore, Eq. (9) is determined as follows.

$$\Phi' = 10^{\left[\frac{(b/D)}{0.03 + 0.42 (b/D)} \right]} \times 10^{-\left[\frac{(b/D)(d/D)}{0.01 + 0.73 (b/D)} \right]} \quad (9')$$

Plotting this Eq. (9') on Fig. 6, the dotted lines are obtained. As a whole, the agreements of Eq. (9') with the observed values are good except in the case of $(b/D)=0.05$.

Accordingly, the following generalized equation is obtained:

$$\frac{Pg_c}{\rho n^3 d^5} = A \cdot B \left(\frac{d^2 n \rho}{\mu} \right)^p \quad (12)$$

where

$$A = 10^{\left[\frac{(b/D)}{0.03 + 0.42 (b/D)} \right]} \quad (12)_1$$

$$B = 10^{-\left[\frac{(b/D)(d/D)}{0.01 + 0.73 (b/D)} \right]} \quad (12)_2$$

$$p = -\left[\frac{(b/D)}{0.17 + \{1.8 + 1.37 (d/D)\} (b/D)} \right] \quad (12)_3$$

Eq. (12) is applicable to the paddles of an arbitrary shape in the region where $(b/D) \geq 0.1$.

To obtain a more accurate result, especially in the region of $(b/D) < 0.1$, it is desirable to use the coefficient A taken from the plot of the dotted line in Fig. 7.

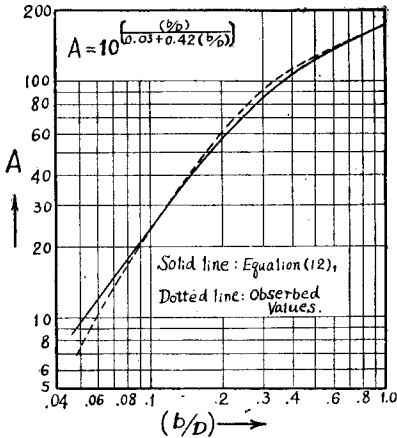


Fig. 7. Coefficient A in Eq. (12) vs (b/D) ratio—Comparison of the values A calc. by Eq. (12)₁ and those obtained from experiment.

4.3. Power equation for a low viscosity range.

$$(Re > 10^4 \sim 10^5 \text{ or more exactly } Re > R_2)$$

In the low viscosity range, the slopes p of the curves are nearly equal to -0.113 as clearly shown by Fig. 2 and 3.

Therefore, Eq. (2) becomes :

$$\phi'' = \left(\frac{Pg_c}{\rho n^3 d^5} \right) \cdot \left(\frac{d^2 n \rho}{\mu} \right)^{0.113} = f'' \left(\frac{d}{D}, \frac{b}{D} \right) \quad (13)$$

By the same procedures used in [4.2], Eq. (13) is determined as follows :

$$\frac{Pg_c}{\rho n^3 d^5} = \frac{(b/D)}{0.05 + 1.05 (b/D)} \cdot \left(\frac{d}{D} \right)^{-1.23} \cdot \left(\frac{d^2 n \rho}{\mu} \right)^{-0.113} \quad (13')$$

The solid lines drawn on Fig. 2 and 3 are the calculated lines of Eq. (5), (12) and (13'). With the exception of $(b/D)=0.05$, good agreements with the observed values are obtained. The dotted lines in the range of medium viscosity shown in Fig. 3 are drawn by using A value taken from the dotted line in Fig. 7 and good agreement with the observed values is obtained.

4.4. Boundary Reynolds number ; R_1 and R_2 .

As mentioned above, the authors obtained empirical equations for three ranges of Reynolds number. The boundary Reynolds number R_1 is varied by the ratios (d/D) and (b/D) , and R_2 may be assumed to vary with the ratio (d/D) .

By the same procedure explained above, the following equations are obtained to determine the boundary Reynolds number.

$$R_1 = 10^{\left[\frac{2.178 - \frac{(1-d/D)(b/D)}{0.02 + 0.58(b/D)}}{0.02 + 0.58(b/D)} \right]} \quad (14)$$

$$R_2 = -3.3 \times 10^4 + 14.1 \times 10^4 (d/D) \quad (15)$$

The chain lines R_1-R_1 and R_2-R_2 drawn on Fig. 2 and 3 correspond to Eq. (14) and (15).

4.5. Method of application of the power equations.

To calculate the power at an arbitrary condition, the following procedures are recommended :

- (1) Calculate the Reynolds number at given conditions and also R_1 , R_2 for a given paddle.
- (2) Compare the Reynolds number with R_1 and R_2 , and decide the range of viscosity. In case of $Re < R_1$, use Eq. (5), in case fo $R_1 \leq Re \leq R_2$, use Eq. (12), and in case of $Re > R_2$, use Eq. (13').
- (3) Calculate the values P , paying careful attention to use consistent units.

When Reynolds number is less than R_1 , but is not far off, i. e., for the range of $R_1/10 < Re < R_1$, the state of agitation is in the transitional range and either Eq. (5) or Eq. (12) does not hold good. These deviations are shown clearly in Fig. 3 in connection with the paddle of larger (d/D) ratio. For this range, N_{P_1} for R_1 is calculated by Eq. (12) and N_{P_2} for $R_1/10$ is calculated by Eq. (5). The approximate value of

N_P for the given Re can be estimated by the following proportional expression:

$$N_P = N_{P_2} - (N_{P_2} - N_{P_1}) \frac{Re - R_1/10}{R_1 - R_1/10} \quad (16)$$

The lines drawn in the transitional range of Fig. 2 and 3 are the calculated lines of Eq. (16).

5. Effect of liquid depth and the correction term for (H/D) .

In the previous experiments, the liquid depth H was held to be equal to the vessel diameter D , i. e., $(H/D)=1$. Then, the effect of liquid depth (H/D) on the power consumption is studied.

The power requirement at an arbitrary liquid depth H , denoted as P_H , is given by multiplying the power P_1 at the ratio of $(H/D)=1$ by a correction term $(H/D)^h$:

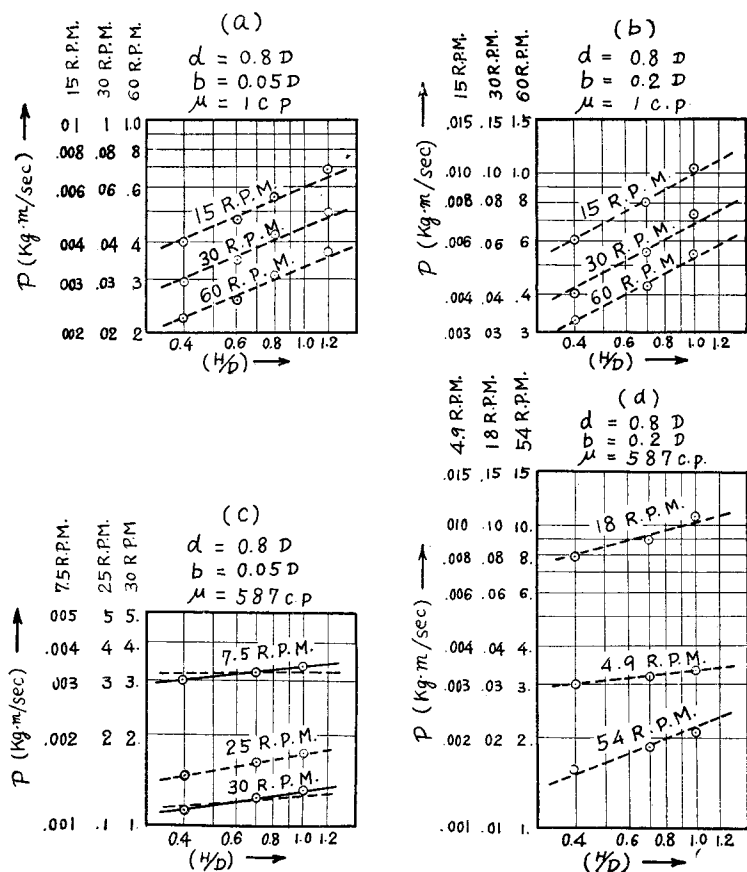


Fig. 8. Effect of the liquid depth on the power consumption in liquids of various viscosities.

$$P_H = P_1 (H/D)^h \tag{17}$$

When the viscosity of liquid is low, for example as low as that of water, P is proportional to $(H/D)^{0.4} \sim (H/D)^{0.55}$, but in the liquid of high viscosity P_H is proportional to $(H/D)^0$. In other words, the power required is independent of liquid depth. Therefore, the exponent h is presumably a function of Reynolds number.

Conditions of Experiments :

Vessel used : $D=585$ mm, $H_P=H/2$, $H/D=1.2, 1.0, 0.8, 0.6, 0.4$

Impeller used : paddle, $\theta=90^\circ$, $n_p=2$

$(d/D)=0.2, 0.5, 0.8$, $(b/D)=0.05, 0.1, 0.2$

Liquid used : water ; 1.0 c. p.

machine oil ; 25.7 c. p., 70~85 c. p. and 580~650 c. p.

With the paddies having the above dimensions, experiments are made to clarify the effect of liquid depth in liquids of various viscosities.

The power consumptions at an equal agitator speed are plotted against (H/D) ratio on a logarithmic paper. For example, the data for $(d/D)=0.8$ are shown by Fig. 8. From these plots, the exponent h in Eq. (17) is determined. The value of exponent h decreases with the increase in viscosity; in some cases as shown by Fig. 8 (d), however, it obviously increases with the speed of agitator.

Also, the exponent h changes with the change in paddle width b , but not with the change in paddle length d . These values of h are taken from Fig. 8 and others (figures omitted) and they are plotted against Reynolds number as shown by the curve A in Fig. 9. In these plots, exponent h changes slightly in the scope of large

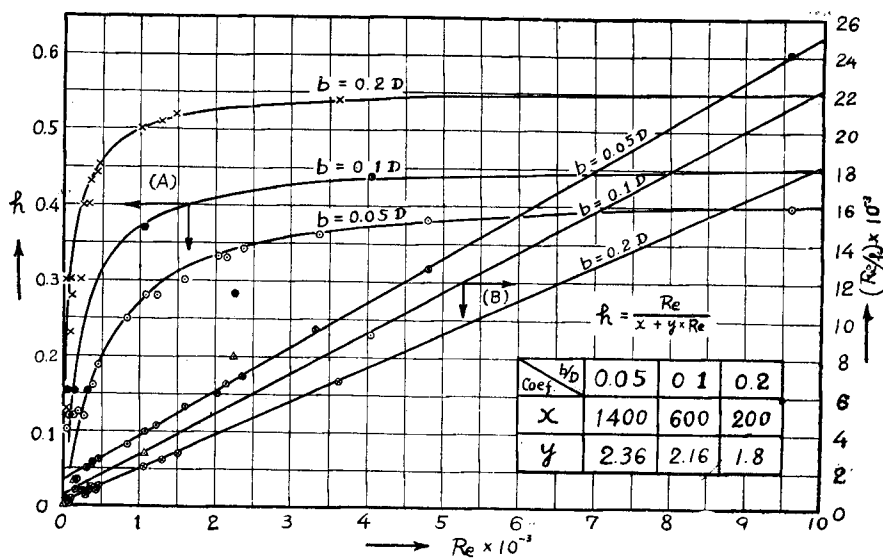


Fig. 9. Variation of the exponents h on the correction term for liquid depth at various Reynolds number.

and medium Reynolds numbers and is nearly equal to those of water; but they decrease suddenly at smaller Reynolds range (about 10^3). Here again, it is assumed that the hyperbolic relation exists. Therefore, the values (Re/h) are calculated and taken as ordinate on the right hand side, then the relation (Re/h) and Re shows nearly a straight line, as shown by the curve B in Fig. 9.

$$h = \left[\frac{Re}{x + yRe} \right] \quad (18)$$

From the slope of the lines in group B , the coefficient y is determined and from the intercepts in ordinate at $Re=0$, the coefficients x is determined. Thus, the following relations are obtained:

$$x = 23.5 (b/D)^{-1.38} \quad (19)$$

$$y = 2.55 - 4 (b/D) \quad (20)$$

Therefore, Eq. (18) is determined as follows:

$$h = \left[\frac{Re}{23.5 (b/D)^{-1.38} + \{2.55 - 4 (b/D)\} Re} \right] \quad (21)$$

The lines calculated by this Eq. (21) are drawn as shown by the dotted lines on Fig. 8. It is apparent that the agreement between the observed data and the calculated lines is satisfactory. As the result, Eq. (17) is determined as follows:

$$P_H = P_1 (H/D) \left[\frac{Re}{23.5 (b/D)^{-1.38} + \{2.55 - 4 (b/D)\} Re} \right] \quad (17')$$

The power P_1 for $(H/D)=1$ can be calculated by Eq. (12) or by Eq. (13') corresponding to the ranges of Reynolds number. In the viscous flow ranges, Eq. (5) is adopted and the ratio of (H/D) does not affect the power value.

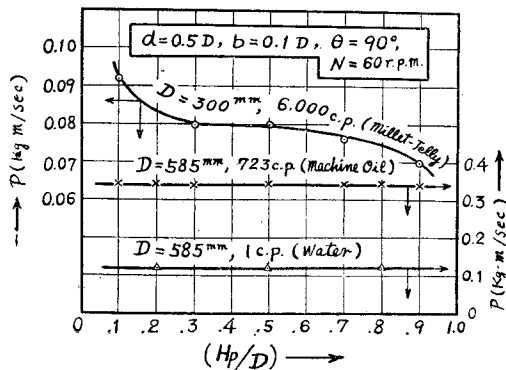


Fig. 10. Effect of the paddle location (H_p) in vertical direction upon power consumption.

6. Effect of the location of paddle on the power consumption and the effect of blade number.

6.1. Single paddle.

The height of the paddle (H_p) located in an agitated vessel has little effect on the power consumption as shown by Fig. 10. It seems that there is a small difference between the power consumed by a paddle near the top $H_p=0.9D$ (or near the bottom $H_p=0.1D$)

and that near the middle height. However, from the practical point of view, these differences are negligible in most cases.

6.2. Multi-stage paddles.

The distance of two or more paddle located in an agitated vessel has little effect on the power data as shown by Fig. 11 and Fig. 12. In Fig. 11, the power consumption for a paddle with double width (Fig. 11 (1)) is equal to the power consumed by two paddles at an arbitrary distance (Fig. 11, (2), (3)). As an extreme case, the power consumed by an impeller having four blades (Fig. 11, (4)) is equal to the power required for a paddle with double width (Fig. 11, (1)). As a result, in the concentric agitation in a same vessel, the power consumed by impellers having equal d and θ is the same, if

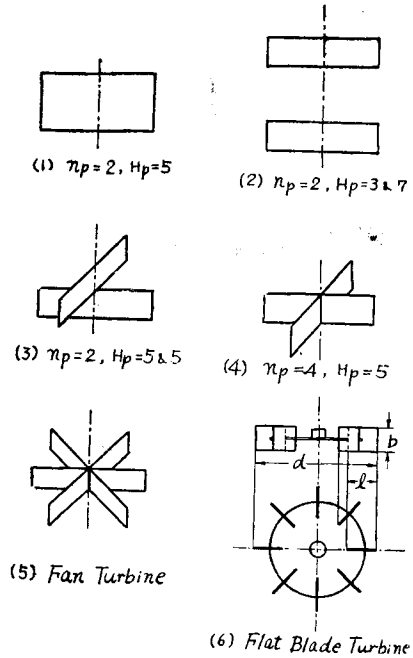


Fig. 11. Impellers having equal power requirements.

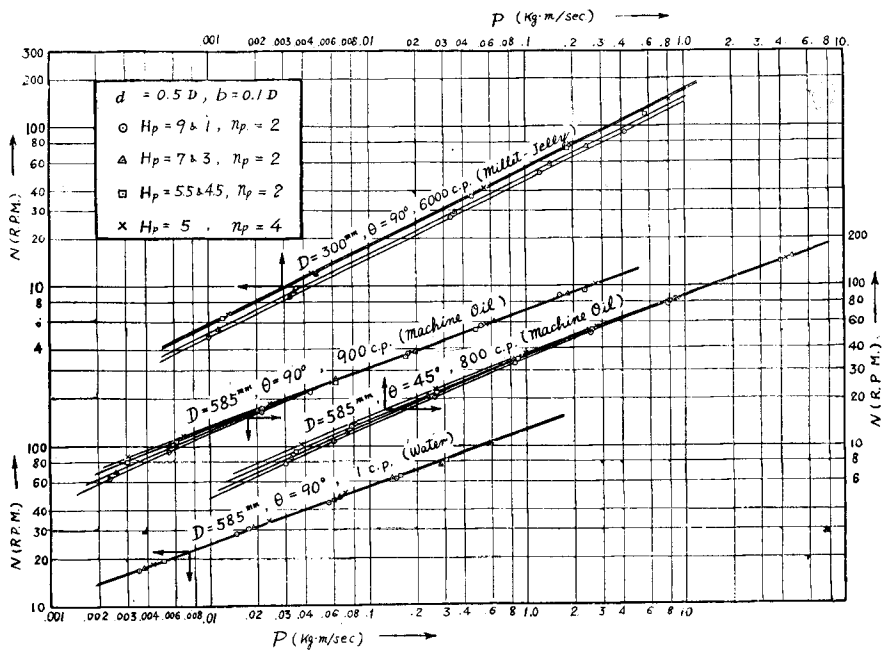


Fig. 12. Power consumed by the two paddles located at various intervals.

$$b \times n_p = \text{constant} \quad (22)$$

It should be noted here that the above Eq. (22) can not be applied to agitation in the baffled vessels.

6.3. Turbine agitator.

Turbine agitator is a sort of impeller shown by Fig. 11 (6). As discussed in a previous report (I),³⁾ in the liquid of low and medium viscosities, the cylindrically rotating zone may extend to the inner side of the turbine blade so that the power consumption of the turbine (6) may be equal to that of the fan turbine with equal blades (5).

From the above discussion, it can be concluded that the power consumptions of the impellers shown in Fig. 11 (1)~(6) are all equal in quantity in the liquids of low and medium viscosities. Further details will be discussed in a succeeding report.

7. Maximum power consumption.

7.1. The fully baffled conditions.

Power consumption in a vessel is increased by insertion of the baffle plates at the tank wall because the circumferential flow of liquid is impeded and the cylindrically rotating zone, discussed in report (I),³⁾ disappears.

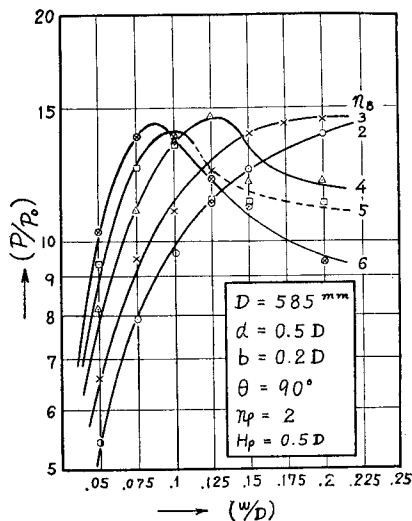


Fig. 13. Diagram showing the power increase accompanied by the increase in baffle width.

By increasing the width of baffles, the ratio of paddle area, which has a larger relative velocity to the liquid, increases and a maximum power is reached. As an example, the variation of power consumption accompanied by the increase in baffle width is shown in Fig. 13. The paddle used have the dimensions of $d=0.5D$, $b=0.2D$, $\theta=90^\circ$ and $n_p=2$, and it is rotated in a tank of $D=585$ mm. The power (P) for baffle plates of width w is compared with the power (P_0) without baffle. The power increases rapidly as the baffle width increases until finally a maximum value is reached, and then decreases somewhat in a larger (w/D) ratio. The maximum power P_{\max} is reached at a smaller (w/D) ratio as the number of baffles is increased. The relative width of baffle plates at which maximum power is attained, can roughly be indicated as follows:

$$(w/D) \times n_B = 0.5 \quad (23)$$

relative width of baffle plates at which maximum power is attained, can roughly be indicated as follows:

This relation is called the "Fully Baffled Condition".

7.2. Baffle width at which the fully baffled condition is reached for various paddles.

The fully baffled condition may vary with paddle length (d) or with paddle width (b). But, judging from the experimental results, baffle width, at which the maximum power is attained, is almost always constant for various paddle sizes as shown by Fig. 14, and Eq. (23) holds good for various paddles.

7.3. The constancy of the P_{max} value for liquids of various viscosities.

The maximum power P_{max} is nearly constant for liquids of various viscosities as reported by J.H. Rushton *et. al.*¹⁾ This result is also ascertained by the author's present experiments as shown by Fig. 3 (curve (1') and (2')).

By the partly baffled conditions, the power values are also constant for liquids of various viscosities as shown by curve (2''). This result is similar to the relation between friction factor and Reynolds number for liquid flow in the pipe lines having various roughness.

7.4. Empirical equation of P_{max} .

From the results of [7.1], [7.2] and [7.3], the conditions at which a maximum power is attained have been determined and it has been found that the value P_{max} can easily be obtained by these experiments carried in water.

The conditions of baffle plate insertion are fixed to be $n_B=6$, $w=0.1D$ (one of the fully baffled conditions) for various paddle, with an exception of a paddle having $d=0.8D$ in which case the baffles of $w=0.075D$ and $n_B=6$ are preferred.

The power data are converted to the N_P values $\left(\frac{P_{max} \cdot g_c}{\rho n^3 d^5}\right)$ and plotting it against (d/D) ratio, Fig. 15 is obtained.

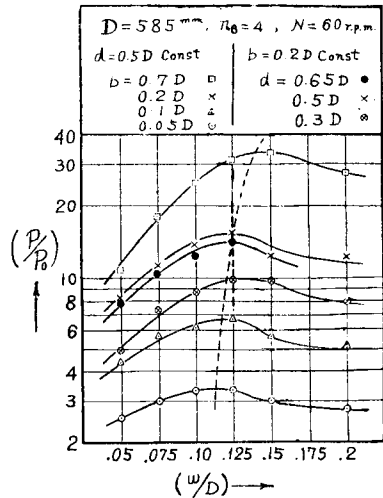


Fig. 14. Diagram showing the baffle width at which max. power is reached.

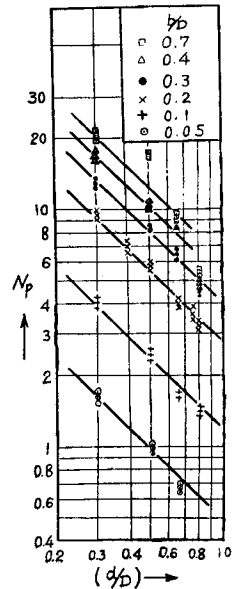


Fig.15. Variation of the N_P value for P_{max} accompanied by the change in (d/D) ratio.

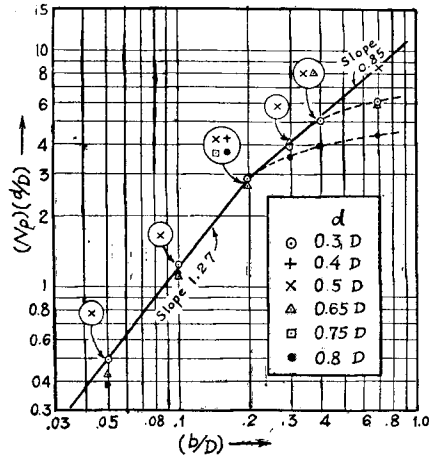


Fig. 16. $N_P(d/D)$ vs (b/D) —
Diagram to be used to determine the coefficient and the exponent in Eq. (24).

From these plots, N_P is expressed as follows:

$$N_P = c(d/D)^{-1} f(b/D) \quad (24)$$

or

$$N_P(d/D) = c \cdot f(b/D) \quad (24')$$

Then the values $N_P(d/D)$ are calculated and plotting it against (b/D) ratio on a logarithmic paper, Fig. 16 is obtained. For large values in (b/D) ratio, deviation from the solid line is large, but as for the proper range of application, the following equations are derived:

for the range of $b=0.05D \sim 0.2D$,

$$d=0.3D \sim 0.8D,$$

$$\frac{P_{\max} \cdot g_c}{\rho n^3 d^5} = 23 (b/D)^{1.27} (d/D)^{-1} \quad (25)$$

and for the range of $b=0.2D \sim 0.4D$, $d=0.3D \sim 0.7D$,

$$\frac{P_{\max} \cdot g_c}{\rho n^3 d^5} = 12 (b/D)^{0.85} (b/D)^{-1} \quad (25')$$

7.5. Power consumption at the start of agitation (Initial power, $P_{\text{init.}}$)

At the moment when a paddle agitator begins to rotate, the total area of the paddle receives resistance of the liquid and the power ($P_{\text{init.}}$) may be equal to the maximum power (P_{\max}) explained above. Once the liquid begins to rotate, the power

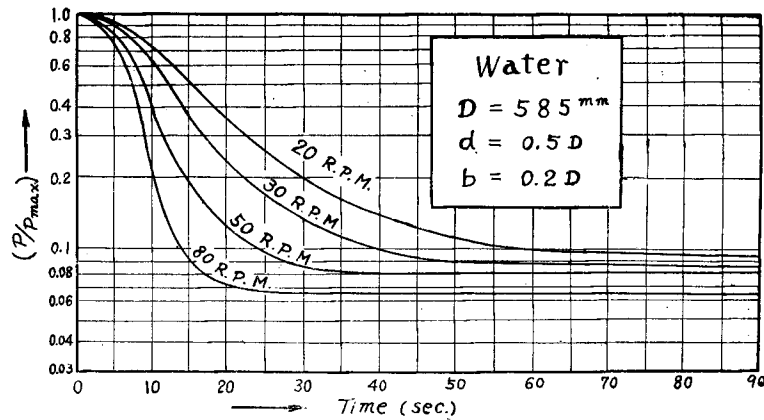


Fig. 17. Power decrease occurring with the lapse of time.

consumption is reduced gradually until finally a smaller power value at a steady state is reached. The process of the change in power ratio ($P/P_{\text{init.}}$) is given in Fig. 17. This initial power is transformed into the power number N_P and plotted on Fig. 3. The agreement between N_P values from $P_{\text{init.}}$ and these from P_{max} is good as shown by the point marked with twofold circle on the curve (2'). Therefore, the following relation is obtained:

$$P_{\text{init.}} = P_{\text{max.}} \quad (26)$$

8. Conclusion.

Empirical equations were obtained to calculate the power consumption of paddle agitators, having arbitrary dimensions, in a vessel containing the liquids of various viscosities.

In the case of concentric agitation without baffle plates, Eq. (5), (12) and (13') are used for three ranges of Reynolds number, respectively.

The effect of liquid depth to power consumption is examined and the correction term to be applied for Eq. (12) and (13') is obtained as Eq. (17').

The power consumption of multi-stage paddles and that of the impeller with various number of blades can now be reduced to the power consumed by a single paddle agitator.

In the fully baffled condition, the power consumption is independent of the viscosity of liquids and can be calculated by Eq. (25) and (25').

Literature Cited

- 1) J. H. Rushton, E. W. Costich and H. J. Everett: Chem. Eng. Progr. **46**, 395, 467 (1950).
- 2) S. Nagata and T. Yokoyama: Memoirs of the Faculty of Engineering, Kyoto University, **17**, No. 4 (1955).
- 3) S. Nagata, N. Yoshioka and T. Yokoyama: Memoirs of the Faculty of Engineering, Kyoto University, **17**, No. 3, 175 (1955).